ISSN 1070-3284, Russian Journal of Coordination Chemistry, 2023, Vol. 49, No. 1, pp. 33–40. © Pleiades Publishing, Ltd., 2023.
Russian Text © The Author(s), 2023, published in Koordinatsionnaya Khimiya, 2023, Vol. 49, No. 1, pp. 36–43.

Rhenium(V) Tris(pyrazolyl)borate Complexes as Ligands in Square Planar Palladium and Platinum Complexes

I. V. Skabitskii[a], *, Yu. Ya. Il'ina[a], and S. S. Shapovalov[a]

[a] *Kurnakov Institute of General and Inorganic Chemistry, Russian Academy of Sciences, Moscow, 119991 Russia*

**e-mail: skabitskiy@gmail.com*

Received May 13, 2022; revised July 5, 2022; accepted July 7, 2022

Abstract—The reactions of $TpReO(S^nC_3H_7)_2$ (Tp = tris(pyrazolyl)borate anion) with acetonitrile complexes $PdCl_2(MeCN)_2$ and $PtI_2(MeCN)_2$ in toluene solutions resulted in the formation of new heterometallic rhenium complexes $TpReO(\mu\text{-}S^nC_3H_7)_2MX_2$ ($MX_2 = PdCl_2$ (**I**), $MX_2 = PtI_2$ (**II**)). A similar complex $TpReO(\mu\text{-}S^nC_3H_7)_2PdI_2$ (**III**) was formed either on treatment of **I** with NaI in dichloromethane or in the reaction of $TpReO(S^nC_3H_7)_2$ with a suspension of PdI_2 in toluene. Complexes **I**–**III** were characterized by IR and NMR spectroscopy and by X-ray diffraction (CCDC nos. 2172225–2172227).

Keywords: rhenium complexes, thiolate complexes, heterometallic complexes, tris(pyrazolyl)borate, X-ray diffraction

DOI: 10.1134/S1070328422700191

INTRODUCTION

The catalyst deactivation during reforming is mainly caused by coke deposition on the catalyst surface. A key effect of the addition of rhenium to a monometallic platinum-based catalyst supported on alumina is increase in the catalyst stability [1]. The addition of chemisorbed sulfur to a catalytic system gives rise to inactive ReS units, which separate large Pt assemblies into smaller ones; as a result, the amount of deposited coke decreases and the hydrogen content in the coke increases [2]. The reaction mechanism also changes: in the case of sulfonated systems, the selectivity of methylcyclopentane conversion to benzene and cyclohexane increases [3]. Thus, platinum–rhenium chalcogenide complexes may be of interest for the preparation of heterogeneous catalysts.

One way for the synthesis of heterometallic clusters is to use complexes containing two terminal thiolate groups as ligands for isolobal metal moieties; particularly, ruthenium [4] and rhodium [5, 6] tris-pyrazolylborate complexes were used to obtain dimers containing also Pd, Pt, Re, and Mo.

However, heterometallic rhenium(V) complexes with the coordinated tris-pyrazolylborate anion and two terminal thiolate ligands $LReO(SR)_2$ ($L = HBPz_3$ or BPz_4, where Pz is pyrazole [7]) have not yet been obtained. Moreover, only few structures are known in which the thiolate complex containing also the terminal oxo ligand is coordinated to another metal via the formation of thiolate bridges [8, 9].

Low reactivity of compounds of this type may be caused by the involvement of lone pairs of sulfur in the additional π-donation to the antibonding π-orbital of the Re–O multiple bond, which is manifested as a considerable shortening of Re–S bonds according to X-ray diffraction data and hindered rotation of thiolate ligands in solution according to NMR data [10]. In this study, we intended to elucidate the conditions under which the complex $TpReO(S^nC_3H_7)_2$, which we obtained, would be coordinated to platinum group metals.

EXPERIMENTAL

All operations related to the synthesis and isolation of products were carried out in anhydrous solvents under a pure argon atmosphere. IR spectra were measured on a Bruker Alpha spectrometer with a Bruker Diamond ATR attachment. ^1H, ^{13}C, and ^{195}Pt NMR spectra were recorded on a Bruker AV 300 instrument; ^1H and ^{13}C NMR chemical shifts were referred to tetramethylsilane; ^{195}Pt chemical shifts were referred to Na_2PtCl_6 in D_2O. $TpReO(S^nC_3H_7)_2$ [10], $PdCl_2(MeCN)_2$ [11], and PdI_2 [12] were synthesized according to published procedures. $PtI_2(MeCN)_2$ was prepared by treating $PtCl_2(MeCN)_2$ with sodium iodide in acetonitrile [13].

Synthesis of $TpReO(\mu\text{-}S^nC_3H_7)_2PdCl_2$ (I). $PdCl_2(MeCN)_2$ (100 mg, 0.38 mmol) was added to a solution of $TpReO(S^nC_3H_7)_2$ (212 mg, 0.38 mmol) in toluene (15 mL). The resulting suspension was stirred at 60°C for 16 h. The brown powder of **I** was isolated

by decantation, washed with toluene and pentane, and dried in vacuum. The yield was 195 mg (70%).

IR (ν, cm^{-1}): 3145 vw, 3123 vw, 3091 vw, 2958 vw.br, 2928 vw, 2868 vw, 2534 vw.br, 1504 w, 1456 vw, 1442 vw, 1407 s, 1390 vw, 1310 vw, 1297 m, 1215 w, 1200 m, 1185 vw, 1173 w, 1120 m, 1106 vw, 1076 vw, 1045 vs, 995 vw, 974 vs, 903 vw, 879 vw, 814 vw, 782 vs, 712 m, 672 vw, 650 w, 616 m.

^{1}H NMR (CD_2Cl_2; 298 K; δ, ppm): 0.89 (t, $^3J_{H–H}$ = 7.35 Hz, 6H, $SCH_2CH_2CH_3$), 1.76 (m, 4H, $SCH_2CH_2CH_3$), 2.79 (ddd, 2H, $SCH_2CH_2CH_3$), 3.07 (ddd, 2H, $SCH_2CH_2CH_3$), 6.43 (t, $^3J_{H–H}$ = 2.4 Hz, 1H), 6.61 (t, $^3J_{H–H}$ = 2.5 Hz, 2H), 7.72 (dd., $^3J_{H–H}$ = 2.3 Hz, $^4J_{H–H} \approx$ 0.5 Hz, 1H), 7.89 (d, $^3J_{H–H}$ = 2.5 Hz, 2H), 8.02 (dd, $^3J_{H–H}$ = 2.5 Hz, $^4J_{H–H} \approx$ 0.6 Hz, 2H), 10.9 (d, $^3J_{H–H}$ = 2.2 Hz, 1H). ^{13}C {^{1}H} NMR DEPT (CD_2Cl_2; 298 K; δ, ppm): 13.23, 26.72 (CH_2), 44.98 (CH_2), 108.65, 109.85, 137.1, 139.70, 147.57, 154.32.

For $C_{15}H_{24}BN_6OS_2Cl_2PdRe$ (M = 743)

Anal. calcd., %:	C, 24.25;	H, 3.25;	N, 11.31
Found, %:	C, 25.07;	H, 3.32;	N, 11.17

The crystals of **I** suitable for X-ray diffraction were obtained by keeping $PdCl_2(MeCN)_2$ in a solution of $TpReO(S^nC_3H_7)_2$ in CH_2Cl_2 at room temperature for a week.

Synthesis of $TpReO(\mu\text{-}S^nC_3H_7)_2PtI_2$ (II). $PtI_2(MeCN)_2$ (45 mg, 0.085 mmol) was added to a solution of $TpReO(S^nC_3H_7)_2$ (48 mg, 0.085 mmol) in toluene (15 mL). The resulting suspension was stirred at 80°C for 3 days. The black powder of **II** was isolated by decantation, washed with toluene and pentane, and dried in vacuum. The yield was 71 mg (83%).

IR (ν, cm^{-1}): 3120 vw, 3089 vw, 3054 vw, 2966 vw, 2925 vw.br, 2864 vw, 2530 vw, 1503 w, 1405 s, 1388 vw, 1310 vw, 1299 m, 1211 w, 1200 vw, 1185 vw, 1177 m, 1119 m, 1071 vw, 1047 vs, 992 vw, 973 s, 913 vw.br, 870 vw, 811 vw, 778 vw, 771 vs, 723 vw, 710 m, 670 vw, 650 w, 613 w, 500 vw, 461 vw, 414 vw.

^{1}H NMR (CD_2Cl_2; 298 K; δ, ppm): 0.84 (t, $^3J_{H–H}$ = 7.34 Hz, 6H, $SCH_2CH_2CH_3$), 1.67 (m, 4H, $SCH_2CH_2CH_3$), 3.06 (ddd, 2H, $SCH_2CH_2CH_3$), 3.44 (ddd, 2H, $SCH_2CH_2CH_3$), 6.35 (t, $^3J_{H–H}$ = 2.4 Hz, 1H), 6.61 (t, $^3J_{H–H}$ = 2.4 Hz, 2H), 7.68 (dd, $^3J_{H–H}$ = 2.4 Hz, $^4J_{H–H} \approx$ 0.7 Hz, 1H), 7.90 (d, $^3J_{H–H}$ = 2.2 Hz, 2H), 8.02 (dd, $^3J_{H–H}$ = 2.5 Hz, $^4J_{H–H} \approx$ 0.7 Hz, 2H), 10.8 (d, $^3J_{H–H}$ = 2.1 Hz, 1H). ^{13}C {^{1}H} NMR DEPT (CD_2Cl_2; 298 K; δ, ppm): 12.77, 27.75 (CH_2), 44.97 (CH_2), 108.71, 109.63, 136.79, 139.56, 147.21, 151.28. ^{195}Pt {^{1}H} NMR −3704.

For $C_{15}H_{24}BN_6OS_2I_2PtRe$ (M = 1014)

Anal. calcd., %:	C, 17.76;	N, 8.29;	H, 2.38
Found, %:	C, 18.42;	N, 8.80;	H, 2.87

Synthesis of $TpReO(\mu\text{-}S^nC_3H_7)_2PdI_2$ (III). A suspension of PdI_2 (33 mg, 0.09 mmol) in a solution of $TpReO(S^nC_3H_7)_2$ (53 mg, 0.09 mmol) in toluene (10 mL) was stirred at 60°C for 16 h. The light brown solution was filtered, the brown powder was washed with toluene and pentane, and extracted with 5 × 5 mL of CH_2Cl_2. The extract was concentrated to 1/4 of the volume and diluted with hexane (5 mL). The finely crystalline black powder that precipitated at −25°C was isolated by decantation, washed with pentane, and dried in vacuum. The yield was 46 mg (54%).

IR (ν, cm^{-1}): 3120 vw, 3090 vw, 2947 vw, 2925 vw, 2865 vw, 2530 vw, 1504 w, 1455 vw, 1441 vw, 1431 vw, 1406 s, 1389 vw, 1311 vw, 1301 m, 1212 m, 1200 w, 1186 vw, 1178 w, 1120 m, 1105 vw, 1073 vw, 1049 vs, 993 vw, 974 vs, 917 vw, 898 vw, 871 vw, 812 vw, 778 vs, 770 vw, 724 vw, 711 s, 670 vw, 651 w, 621 vw, 614 w.

^{1}H NMR (CD_2Cl_2; 298 K; δ, ppm): 0.86 (t, $^3J_{H–H}$ = 7.35 Hz, 6H, $SCH_2CH_2CH_3$), 1.59 (m, 2H, $SCH_2CH_2CH_3$), 1.74 (m, 2H, $SCH_2CH_2CH_3$), 3.04 (ddd, 2H, $SCH_2CH_2CH_3$), 3.45 (ddd, 2H, $SCH_2CH_2CH_3$), 6.36 (t, $^3J_{H–H}$ = 2.4 Hz, 1H), 6.60 (t, $^3J_{H–H}$ = 2.4 Hz, 2H), 7.69 (dd, $^3J_{H–H}$ = 2.4 Hz, $^4J_{H–H} \approx$ 0.7 Hz, 1H), 7.91 (d, $^3J_{H–H}$ = 2.2 Hz, 2H), 7.99 (dd, $^3J_{H–H}$ = 2.5 Hz, $^4J_{H–H} \approx$ 0.7 Hz, 2H), 10.5 (d, $^3J_{H–H}$ = 2.1 Hz, 1H). ^{13}C NMR {^{1}H} DEPT (CD_2Cl_2; 298 K; δ, ppm): 12.99, 27.15 (CH_2), 46.06 (CH_2), 108.19, 109.58, 136.79, 139.40, 147.31, 153.34.

X-ray diffraction study was carried out on a Bruker APEX II CCD diffractometer. The absorption corrections were applied by multiple measurement of equivalent reflections using the SADABS program [14]. The structures of **I**–**III** were solved by direct methods and refined by least-squares calculations on F^2 in the anisotropic approximation for non-hydrogen atoms using SHELX-2014 [15] and OLEX2 [16] program packages. The positions of H atoms were calculated geometrically. In structures of **II** and **III** containing independent molecules related in pairs by a translation close to (1/4, 0, 1/2), constraints on the equality of thermal parameters between equivalent atoms were applied to light atoms of the pyrazolate ligands.

The crystallographic data and structure refinement parameters for **I**–**III** are summarized in Table 1; selected bond lengths and bond angles are given in Table 2.

Table 1. Crystallographic data and structure refinement details for **I**–**III**

Parameter	Value		
	I	**II**	**III**
Molecular formula	$C_{60}H_{96}B_4N_{24}O_4S_8Cl_8Pd_4Re_4$	$C_{15}H_{24}BN_6OS_2I_2PtRe$	$C_{15}H_{24}BN_6OS_2I_2PdRe$
M	2971.32	1014.42	925.73
Radiation (λ, Å)		MoK_α (λ = 0.71073)	
Measurement temperature, K	100	100	100
System	Monoclinic	Monoclinic	Monoclinic
Space group	$P2_1/c$	$P2_1/c$	$P2_1/c$
a, Å	18.6659(9)	35.0751(13)	34.9887(18)
b, Å	15.7179(9)	16.1705(6)	16.2134(8)
c, Å	17.8020(10)	17.7065(7)	17.7636(9)
α, deg	90	90	90
β, deg	118.456(4)	93.3590(10)	93.548(2)
γ, deg	90	90	90
V, Å^3	4591.9(5)	10025.6(7)	10057.7(9)
Z	2	16	16
ρ(calcd.), g/cm^{-3}	2.149	2.688	2.445
μ, mm^{-1}	6.485	13.050	8.165
F(000)	2848.0	7360.0	6848.0
Scanning range on θ, deg	3.588–59.206	2.774–54.3	3.404–54
Scan mode		ω	
No. of unique reflections (N_1) (R_{int})	12883 (0.0789)	22208 (0.1180)	21965 (0.1013)
No. of reflections with $I > 2\sigma(I)$ (N_2)	12276	14508	15148
No. of refined parameters	529	1005	1053
GOOF (F^2)	1.080	1.147	1.137
R_1 for N_2	0.0289	0.0389	0.0399
wR_2 for N_1	0.0597	0.0929	0.1094
$\Delta\rho_{max}/\Delta\rho_{min}$, e Å^{-3}	2.58/–1.37	3.26/–2.88	2.23/–1.89

The atom coordinates and other crystal structure parameters of **I**–**III** are deposited with the Cambridge Crystallographic Data Centre (nos. 2172225–2172227, respectively; http://www.ccdc.cam.ac.uk/data_request/cif).

Quantum chemical calculations were carried out within the framework of density functional theory using the ORCA 5.03 program package [17]. The geometry of the complexes was optimized using the PBE functional [18, 19] with all electron split valence double def2-SVP basis set [20] using the D3BJ empirical dispersion correction [21, 22]. The activation energy was calculated using the PBE0 hybrid functional [23] with split valence triple def2-TZVP basis set [20]. The electron density was calculated using scalar relativistic ZORA formalism [24, 25] in an all-electron split valence triple basis set adjusted for this method [26, 27]. Topological analysis of electron density was carried out using the AIMAll program [28].

RESULTS AND DISCUSSION

The reaction of $TpReO(S^nC_3H_7)_2$ with palladium acetonitrile complexes $PdCl_2(MeCN)_2$ in toluene at 60°C results in the precipitation of the new complex $TpReO(\mu\text{-}S^nC_3H_7)_2PdCl_2$ (**I**). A similar reaction with $PtCl_2(MeCN)_2$ does not proceed at 80°C, while on heating to 100°C, the reaction gives $TpReOCl_2$, which was identified by TLC using comparison with a reference sample, as a mixture with a bright green complex (presumably, $TpReOCl(S^nC_3H_7)$, similar to the

Table 2. Bond lengths and bond angles for the structures of complexes **I**–**III**

Bond	$TpReO(SC_3H_7)_2$ [10]	**I**	**II**	**III**
	d, Å			
Re–O	1.697(1)	1.678(4)	1.668(7)	1.685(6)
Re–S	2.3045(5)	2.361(1)	2.390(3)	2.387(2)
	2.3018(5)	2.394(1)	2.385(3)	2.377(2)
Re–N (*trans* to O)	2.268(2)	2.252(4)	2.262(8)	2.264(7)
Re–N (*trans* to S)	2.143(2)	2.101(4)	2.095(8)	2.107(7)
	2.175(2)	2.127(4)	2.093(9)	2.109(7)
M–S		2.284(1)	2.310(3)	2.329(2)
		2.300(1)	2.310(3)	2.329(2)
M–X		2.326(2)	2.6090(8)	2.6006(8)
		2.310(2)	2.6007(9)	2.5914(9)
Angle	ω, deg			
ReSC	115.63(7)	120.1(2)	110.4(4)	110.2(3)
	112.36(6)	113.8(2)	112.4(4)	112.5(3)
ReSM		98.34(5)	98.4(1)	97.77(8)
		96.98(5)	98.5(1)	98.05(8)
ReSRe	89.34	75.85(5)	78.29(9)	79.11(8)
SMS		79.24(5)	81.45(9)	81.27(8)

known TpReOCl(S^{t}Bu) [10]). The platinum iodide complex $PtI_2(MeCN)_2$ proved to be more reactive: it reacts with $TpReO(S^nC_3H_7)_2$ at 80°C to give $TpReO(\mu\text{-}S^nC_3H_7)_2PtI_2$ (**II**) in a high yield. The starting palladium acetonitrile complex $PdI_2(MeCN)_2$ is unstable; therefore, $TpReO(\mu\text{-}S^nC_3H_7)_2PdI_2$ (**III**) can be obtained by the reaction of $TpReO(S^nC_3H_7)_2$ with amorphous PdI_2 in toluene or by exchange of the halide substituents on treatment of complex **I** with NaI in CH_2Cl_2.

It is noteworthy that an attempt to carry out similar reaction for the nickel iodide complex $NiI_2(MeCN)_2$ leads only to NiI_2 without coordination of the rhenium compound.

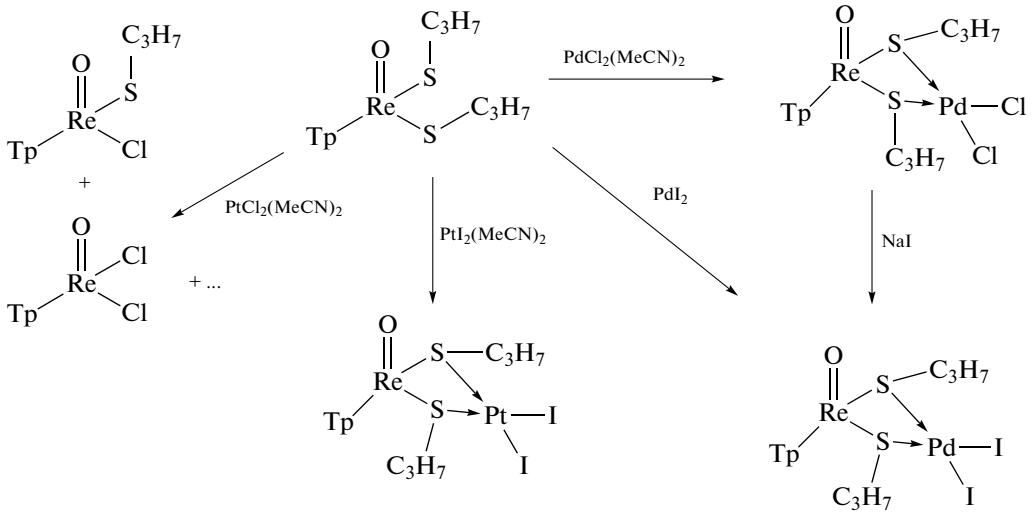

The three new complexes have very similar spectral characteristics. The coordination of the MX_2 moiety leads to a considerable shift of the B–H vibration frequency (2534 cm^{-1} for X = Cl, 2530 cm^{-1} for X = I) to shorter wavelength in the solid phase with respect to that in the starting compound (2479 cm^{-1}). Appar-

ently, this shift is largely associated with the environment of molecules in the crystal, since this difference for solutions in CH_2Cl_2 is much smaller (2507 cm^{-1} for $TpReO(S^nC_3H_7)_2$, 2525 cm^{-1} for complexes **I**–**III**). The DFT calculation of the vibrational frequencies shows a shift by 17 cm^{-1} in the same direction. The intense band assigned to the Re–O vibrations also markedly shifts (from 941 to 973 cm^{-1}) [29], which is in reasonable agreement with the assumed decrease in the additional π-donation from sulfur atoms to the antibonding Re–O orbitals in which one lone pair of each sulfur atom is involved in binding to the second metal. However, note that according to DFT data, the same spectral range also contains bending modes of pyrazolate rings, one of which is in close contact with the second metal.

The ^1H and ^{13}C NMR spectra of complexes **I**–**III** are virtually identical. The major difference from the spectrum of the starting complex is the considerable downfield shift of the signal of one pyrazole proton located in the *trans*-position to the Re–O bond (to 10.5–10.9 ppm compared to initial 7.79 ppm). Furthermore, at room temperature, the spectra of **I**–**III** do not show indications of dynamic processes. This suggests that the conformation of the ReS_2M ring observed in the crystal is retained in solution.

It is noteworthy that an attempt to dissolve the complexes in d^6-DMSO induces fast decomposition; only some of the signals in the spectra of the resulting mixture can be assigned to the initial rhenium complex. Apparently, apart from the displacement of the thiolate chelate from the Pd or Pt coordination sphere, polar DMSO also accelerates the halide and thiolate ligand exchange between the metals, which gives rise to a complex mixture of compounds.

The structure of the complexes was determined by X-ray diffraction. The structure of **I** contains two independent molecules, while isostructural complexes **II** and **III** contain four independent molecules linked in pairs by a non-crystallographic translation close to (1/4, 0, 1/2). The structures of one independent molecule in **I** (Fig. 1b) and all four molecules in **II** and **III** are almost identical. The coordination of the second metal leads to a considerable elongation of Re–S bonds (2.361(1)–2.394(1) Å) in comparison with the initial length (2.3018(5), 2.3045(5) Å). It is of interest that both the longest and shortest distances are observed in one independent molecule of **I** (Fig. 1a), the only one molecule in which the C–C bond of the propyl group located near to sulfur has a different conformation. The sulfur atom with the short Re–S bond also has a shorter S–Pd bond (2.284(1); 2.300(1)–2.329(2)Å in other molecules of structures **I**–**III**), while its ReSC angle (120.1(2)°) is even greater than that in the initial complex (115.63(7)°, 112.36(6)°); meanwhile, the other ReSC angles in structures **I**–**III** are somewhat smaller than those in the initial complex (110.2(3)°–113.8(2)°). Apart from some shortening of the Re–O bond, these changes in the geometric parameters are in good agreement with the assumption that coordination of the second metal would decrease the π-donation from sulfur to the antibonding Re–O orbitals.

It is noteworthy that in all independent molecules of **I**–**III**, the ReS_2M ring has the same conformation in which both thiolate ligands are located in the anti-position to the Re–O bond, while the MX_2 moiety deviates in the same direction, thus forming the short M...H contact (2.660–2.738 Å) with the pyrazolate ring. This may be the key factor responsible for the characteristic changes in the IR and NMR spectra of complexes **I**–**III** in comparison with the initial spectrum.

DFT calculation of the energies of possible conformers of complex **I** results in the lowest energy for the conformer observed by X-ray diffraction. The other configurations of thiolate ligands with respect to the ReS_2M ring are 6.5 and 19.4 kcal/mol higher in energy, while the minima in which the $PdCl_2$ group deviates from the pyrazolate ring are not detected at all.

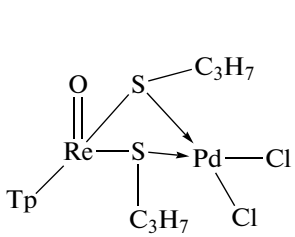

0.0

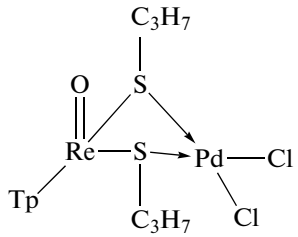

6.5

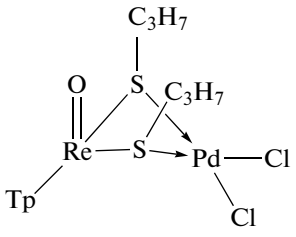

19.4

Analysis of the topology of the calculated electron density of complex **I** (Fig. 2) shows not only the presence of Pd–H bond path, but also a delocalization index (0.083) that is relatively high for a non-covalent

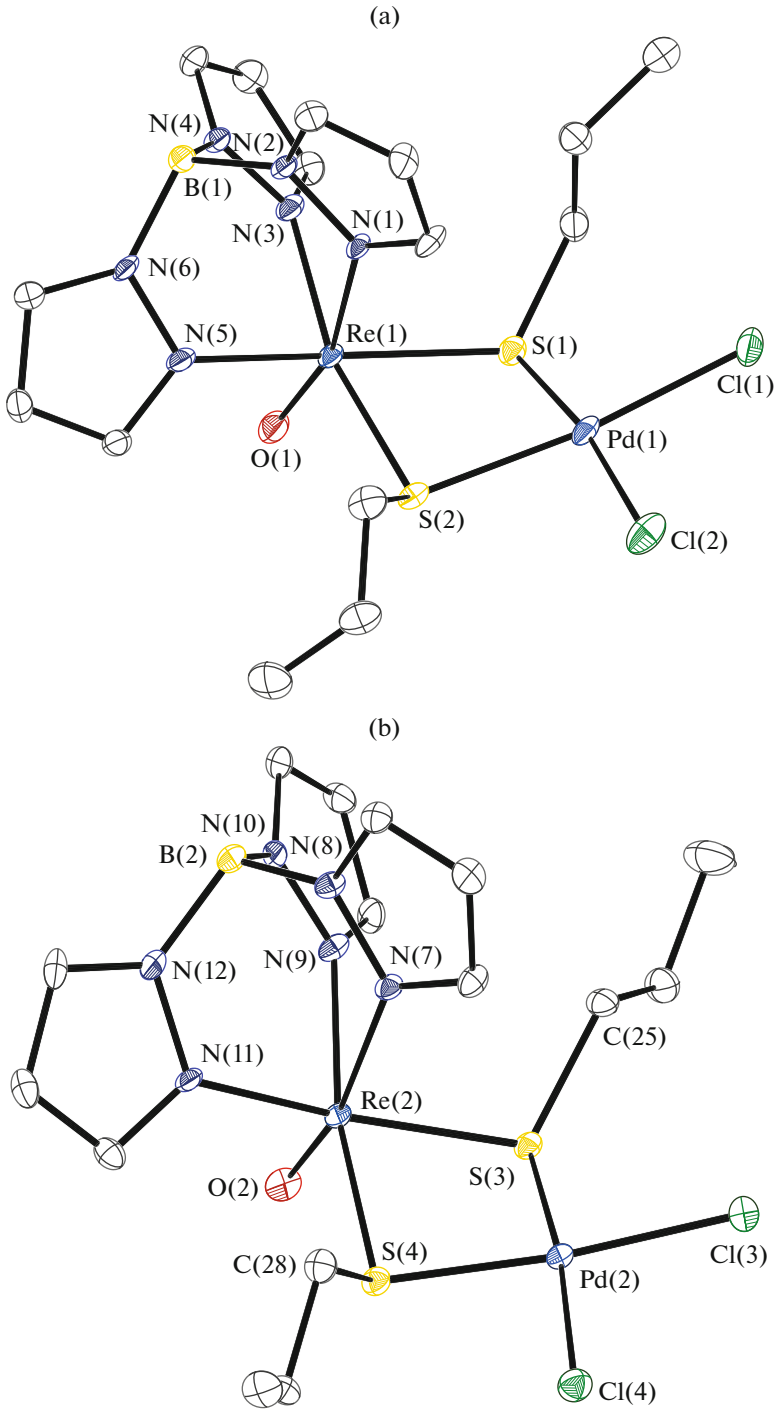

Fig. 1. Molecular structure of **I**: independent molecules with (a) different and (b) identical conformations of propyl groups.

interaction. The Pd–H interaction energy estimated from the potential energy density in the bond critical point [30] is 4.3 kcal/mol.

Thus, we demonstrated the possibility of coordination of rhenium(V) tris-pyrazolylborate complex as a chelating ligand to thiolate ligands. The resulting heterometallic complexes are stable in non-coordinating solvents, but decompose on dissolution in DMSO.

ACKNOWLEDGEMENTS

The studies were performed using equipment of the Center for Collective Use of Physical Investigation Meth-

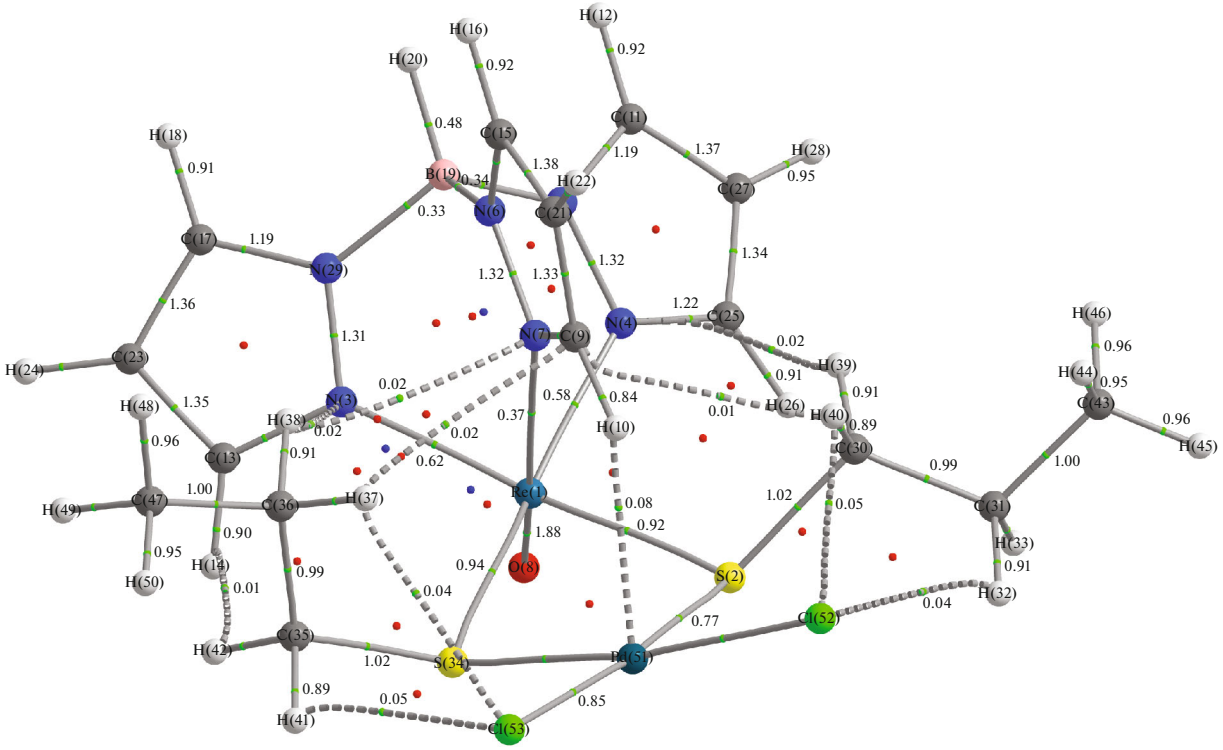

Fig. 2. Molecular graph of complex **I** with indicated positions of critical points and bond paths. Delocalization indices are given for the bond critical points.

ods of the Kurnakov Institute of General and Inorganic Chemistry, Russian Academy of Sciences.

FUNDING

This study was supported by the Russian Science Foundation (grant no. 18-73-10206).

CONFLICT OF INTEREST

The authors declare that they have no conflicts of interest.

REFERENCES

1. Xiao, J. and Puddephatt, R.J., *Coord. Chem. Rev.*, 1995, vol. 143, p. 457.
2. Augustine, S.M., Alameddin, G.N., and Sachtler, W.M.H., *J. Catal.*, 1989, vol. 115, no. 1, p. 217.
3. Dees, M.J., Bol, M.H.B., and Ponec, V., *Appl. Catal.*, 1990, vol. 64, p. 279.
4. Mizobe, M. and Hosomizu, M. Hidai, *Inorg. Chim. Acta*, 1998, vol. 273, p. 238.
5. Misumi, Y., Seino, H., and Mizobe, Y., *Inorg. Chim. Acta*, 2009, vol. 362, p. 4409.
6. Nagao, S., Seino, H., Hidai, M., et al., *Dalton Trans.*, 2005, p. 3166.
7. Lail, M., Pittard, K.A., and Gunnoe, T.B., *Adv. Organomet. Chem.*, 2008, vol. 56, p. 95.
8. Arikawa, Y., Kawaguchi, H., Kashiwabara, K., et al., *Inorg. Chem.*, 1999, vol. 38, p. 4549.
9. Pinder, T.A., Montalvo, S.K., Hsieh, Ch.H., et al., *Inorg. Chem.*, 2014, vol. 53, p. 9095.
10. Skabitskii, I.V., Sakharov, S.G., Pasunskii, A.A., et al., *Russ. J. Coord. Chem.*, 2019, vol. 45, p. 539. https://doi.org/10.1134/S1070328419080086
11. Rimoldi, M., Ragaini, F., Gallo, E., et al., *Dalton Trans.*, 2012, vol. 41, p. 3648.
12. Thiele, G., Brodersen, K., Kruse, E., et al., *Naturwissenschaften*, 1967, vol. 54, p. 615.
13. Rochon, F.D. and Fleurent, L., *Inorg. Chim. Acta*, 1988, vol. 143, p. 81.
14. *SADABS (version 2008/1)*, Madison: Bruker AXS Inc., 2008.
15. Sheldrick, G.M., *Acta Crystalogr., Sect. A: Found. Crystallogr.*, 2008, vol. 64, p. 112.
16. Dolomanov, O.V., Bourhis, L.J., Gildea, R.J., et al., *J. Appl. Crystallogr.*, 2009, vol. 42, p. 339.
17. Neese, F., *Wires Computational Molecular Science*, 2012, vol. 2, no. 1, p. 73.
18. Perdew, J.P., Burke, K., and Ernzerhof, M., *Phys. Rev. Lett.*, 1996, vol. 77, p. 3865.
19. Perdew, J.P., Burke, K., and Ernzerhof, M., *Phys. Rev. Lett.*, 1997, vol. 78, p. 1396.

20. Weigend, F. and Ahlrichs, R., *Phys. Chem. Chem. Phys.*, 2005, vol. 7, p. 3297.
21. Grimme, S., Ehrlich, S., and Goerigk, L., *J. Comput. Chem.*, 2011, vol. 32, p. 1456.
22. Grimme, S., Antony, J., Ehrlich, S., and Krieg, H., *J. Chem. Phys.*, 2010, vol. 132, p. 154104.
23. Adamo, C. and Barone, V., *J. Chem. Phys.*, 1999, vol. 110, p. 6158.
24. van Lenthe, E., Baerends, E.J., and Snijders, J.B., *J. Chem. Phys.*, 1993, p. 4597.
25. van Wüllen, C., *J. Chem. Phys.*, 1998, vol. 109, p. 392.
26. Rolfes, J.D., Neese, F., and Pantazis, D.A., *J. Comput. Chem.*, 2020, vol. 41, p. 1842.
27. Pantazis, D.A., Chen, X.Y., Landis, C.R., and Neese, F., *J. Chem. Theory Comput.*, 2008, vol. 4, p. 908.
28. *AIMAll (version 19.10.12)*, Todd A. Keith, TK Gristmill Software, Overland Park KS, 2019. http://aim.tkgristmill.com/references.html.
29. Degnan, I.A., Behm, J., Cook, M.R., and Herrmann, W.A., *Inorg. Chem.*, 1991, vol. 30, p. 2165.
30. Espinosa, E., Molins, E., and Lecomte, C., *Chem. Phys. Lett.*, 1998, vol. 285, p. 170.

Translated by Z. Svitanko